The existence of non-axisymmetric bilayer vesicle shapes predicted by the bilayer couple model

Vera Kralj-Iglič [1], Saša Svetina [1, 2], Boštjan Žekš [1, 2]

[1] Institute of Biophysics, Medical Faculty, Lipičeva 2, 61105 Ljubljana, Slovenia
[2] J. Stefan Institute, Jamova 39, 61000 Ljubljana, Slovenia

Abstract. The existence of non-axisymmetric shapes with minimal bending energy is proved by means of a mathematical model. A parametric model is used; the shapes considered have an elliptical top view whilst their front view contour is described using Cassini ovals. Taking into account the bilayer couple model, the minimization of the membrane bending energy is performed at a constant membrane area A, a constant enclosed volume V and a constant difference between the two membrane leaflet areas ΔA. It is shown that for certain sets of A, V and ΔA the non-axisymmetric shapes calculated with the use of the parametric model have lower energy than the corresponding axisymmetric shapes obtained by the exact solution of the general variational problem. As an exact solution of the general variational problem for non-axisymmetric shapes would yield even lower energy, this indicates the existence of non-axisymmetric shapes with minimal bending energy in a region of the V/ΔA phase diagram.

Introduction

Phospholipid vesicles exhibit various shapes depending on the properties of the membrane and on the enclosed volume. The diversity of the observed shapes includes, for example, spheres, biconcave discs, cup shapes, and shapes with different protrusions or invaginations (Lipowsky 1991). Studies of such systems lead to the conclusion that the shape of a phospholipid bilayer vesicle can be described theoretically by minimization of the membrane elastic energy. The procedure of minimization of the membrane bending energy was first applied for the determination of the equilibrium shape of human erythrocytes by Canham (1970). A triparametric model was used,

where the vesicle front view contour was described by the Cassini function whilst its top view was taken to be a circle, as only shapes having axial symmetry were taken into account. It was found that under normal conditions the equilibrium shape of an erythrocyte of a given membrane area and a given enclosed volume was a biconcave disc. Deuling and Helfrich (1976) minimized the membrane bending energy by exactly solving a general variational problem for axisymmetric shapes. The variational problem was expressed by the Euler equations for the two principal curvatures, subject to the constraints regarding the membrane area and the enclosed volume. Deuling and Helfrich (1976) also introduced the concept of the spontaneous curvature of the membrane as a model parameter. By varying the spontaneous membrane curvature and the vesicle volume at constant membrane area, different cup shaped, stomatoid, discoid, and dumbbell axisymmetric equilibrium shapes were obtained.

According to the bilayer couple model (Evans 1974; Sheetz and Singer 1974) the phospholipid membrane is considered to consist of two leaflets which are free to slide over each other while staying tightly together along the whole membrane area. It is an essential feature of the model that each layer responds differently to environmental changes, causing different changes of the leaflet areas and thereby changes of the vesicle shape. The difference of the two membrane leaflet areas was theoretically related to the shape change (Svetina et al. 1982; Svetina and Žekš 1989). Svetina and Žekš (1989) solved the Euler equations for the principal curvatures for the axisymmetric shapes. The Euler equations were subject to the constraints requiring fixed values for the average membrane area A, the vesicle volume V and the difference between the two membrane leaflet areas ΔA. Thus many different shapes, including discocytes, cup-shaped cells, pear-shaped cells, dumbbells and cells with spherical protrusions and invaginations were obtained. It was found that at low values of ΔA the calculated equilibrium shapes exhibited invaginations. As ΔA increased, discoid shapes were favored while for high values of ΔA the equilibrium shapes exhibited protrusions. By varying ΔA at constant

A and V, the dependence of the obtained membrane bending energy on ΔA exhibited several local minima. The minima pertaining to the higher values of ΔA corresponded to prolate shapes while the minima pertaining to the lower values of ΔA corresponded to oblate shapes.

Until recently, theoretical studies were restricted to shapes having axial symmetry. Experimental observations do, however, also show non-axisymmetric shapes. Cells having elliptical symmetry were found in the blood of some animals, such as the llama (Khodadad and Weinstein 1983) and in the blood of patients with some hereditary disorders of membrane structure and function (Palek 1987). It was also observed by Hotani (1984) that the shapes of the vesicles prepared from phospholipids and cholesterol exhibit axial as well as polygonal symmetries with $n = 2, 3, 4$ as the vesicle top view is correspondingly deformed from the circle. These shapes were described theoretically by Sekimura and Hotani (1991) by minimizing the membrane bending energy at fixed membrane area and fixed vesicle volume. A parametric model was used, where the vesicle front view contour was desribed by the Cassini function whilst its top view was obtained by deforming a circle into a polygonal shape by means of a trigonometric function. Within such a parametric model it was found that the equilibrium shapes having a large excess area are non-axisymmetric. The existence of non-axisymmetric shapes was theoretically predicted within the spontaneous curvature model (Peterson 1985) where it was shown that the axisymmetric shapes are infinitesimally unstable for some values of model parameters. Following general conclusions for the nearly spherical vesicles (Peterson 1989) it was predicted (Seifert et al. 1991) that non-axisymmetric shapes must exist within the bilayer couple model. These shapes were predicted to exist in the gap between the prolate axisymmetric shapes composed of a cylinder and two spherical caps, and oblate axisymmetric shapes with sharp edges on the equatorial plane. However, it remained an open question as to how far this region of stable non-axisymmetric shapes extends into the prolate and oblate axisymmetric regions. The existence of non-axisymmetric shapes within the bilayer couple model was actually proven for nearly spherical shapes (Heinrich et al. 1992); the variational problem was solved when the shape of vesicles was expanded in terms of spherical harmonics and the membrane bending energy was minimized with respect to the expansion coefficients. It was shown that for ΔA ranging between the oblate and the prolate axisymmetric shapes with the minimal energy values, elliptically deformed spheres exhibited lower membrane bending energy than the corresponding energetically lowest axisymmetric shape.

It is our aim to determine whether within the bilayer couple bending energy model there do exist non-axisymmetric shapes which differ markedly from the sphere. It is our intention to estimate the conditions under which equilibrium non-axisymmetric shapes could be expected, i.e. the conditions under which a non-axisymmetric equilibrium shape has lower energy than the corresponding axisymmetric shape. While the solution of the general variational problem for axisymmetric shapes was derived by Deuling and Helfrich (1976), a corresponding proper generalization for non-axisymmetric shapes leading to the Euler equations in two dimensions has not yet been developed. However, the existence of non-axisymmetric shapes can also be determined by employing a parametric model, provided that the non-axisymmetric shape calculated by such a model has lower energy than the corresponding axisymmetric shape obtained by the solution of the general variational problem.

The parametric model introduced here is restricted to simple closed surfaces having mirror symmetry with respect to the $x = 0$, $y = 0$ and $z = 0$ planes because such shapes were shown to be the equilibrium shapes for nearly spherical vesicles (Heinrich et al. 1992). The vesicle top view is taken to be an ellipse. Such shapes are referred to as elliptical. Elliptical shapes were chosen because elliptical erythrocytes were observed experimentally (Palek 1987; Khodadad and Weinstein 1983) and because the calculated equilibrium shapes of nearly spherical vesicles are elliptical (Heinrich et al. 1992). For the side view contour, a parametric approach is employed by using the Cassini function (determined by three characteristic parameters) which qualitatively corresponds to the observed shapes for the conditions we are considering (Canham 1970). The equilibrium vesicle shape is obtained by determining the values of the model parameters by minimizing the membrane bending energy. The parametric model described is presented in more detail because it could serve as an appropriate tool in the analyses of related experimental data.

Theory

The vesicle shape is determined by minimizing its membrane bending energy

$$W_b = \frac{k_c}{2} \int_A (C_1 + C_2)^2 \, dA, \tag{1}$$

where k_c is the membrane bending constant, C_1 and C_2 the two principal curvatures and dA the area element. The integration is performed over the entire membrane area A. If R_s is the radius of the sphere with this membrane area,

$$R_s = (A/4\pi)^{1/2}, \tag{2}$$

the dimensionless curvatures are $c_1 = R_s C_1$ and $c_2 = R_s C_2$. All other quantities are also expressed in dimensionless form. It is assumed that the relative membrane area $a = A/(4\pi R_s^2)$ is fixed

$$\int da = 1, \tag{3}$$

that the relative volume $v = V/(4\pi R_s^3/3)$ is fixed (where V is the volume of the vesicle),

$$\int dv = v, \tag{4}$$

and that the relative difference between the areas of the two membrane leaflets is fixed

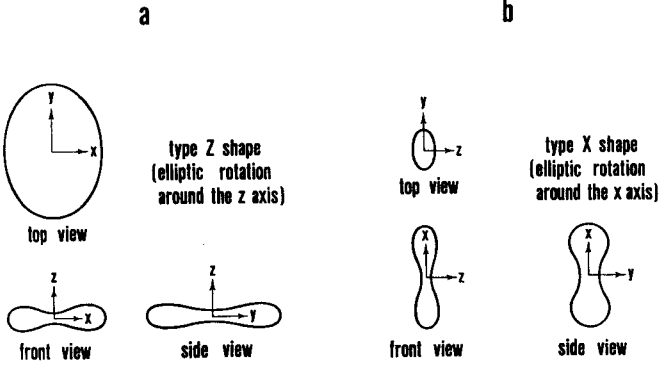$$\frac{1}{2} \int (c_1 + c_2) \, da = \Delta a, \tag{5}$$

a   b

Fig. 1a, b. Cross sections of a vesicle in all three perpendicular planes. a type Z shape, b type X shape. The front view vesicle contour is determined by the Cassini function characterized by the parameters $\alpha = 0.89$, $\beta = 0.68$ and $\gamma = 0.90$ (Eq. (7)) while the vesicle top view is an ellipse with semiaxis ratio $\vartheta = 1.3$

where $\Delta a = \Delta A/8\pi R_s h$ and h is the distance between the two membrane leaflet neutral surfaces. The bending energy is expressed relative to the bending energy of the sphere, $w_b = W_b/8\pi k_c$,

$$w_b = \frac{1}{4}\int (c_1 + c_2)^2 \, da. \tag{6}$$

To generate the shape of the vesicle, a curve $z = f(x)$ describing the vesicle contour in the $y = 0$ plane is chosen to be the Cassini function, as modified by Canham (1970)

$$f(x) = \pm \beta [(\gamma^4 + 4\alpha^2 x^2)^{1/2} - \alpha^2 - x^2]^{1/2}, \tag{7}$$

where α, β and γ are the characteristic parameters and $\pm$ accounts for the symmetry of the contour with respect to the x axis. The ratio α/γ can vary between 0 and 1 while the corresponding contour varies from an ellipse to a lemniscate (shape A in Fig. 5). The parameter β distorts the curve proportionally in the z direction. The parameters α and γ give the maximal extension of the curve in the x direction $\pm\sqrt{\alpha^2 + \gamma^2}$.

The curve (Eq. (7)) can be rotated around its symmetry axes z or x, respectively, giving axisymmetric surfaces which determine the shape of the vesicle. However, if the axisymmetric shape is deformed so that its top view is an ellipse, the shape obtained is elliptical. Two types of

shapes (Z and X, referring to the particular axis of rotation) are considered (Fig. 1). The vesicle surface is expressed by the vector $R^i = (x, y, z(x, y))$ where x, y and z are normalized with respect to R_s and $i = Z, X$. The relative surface area element is given by the expression $da = \frac{1}{4\pi}(EG - F^2)^{1/2}\, dx\, dy$ where the meaning of E, F and G is explained in the Appendix. The relative volume element is given by the expression $dv = 2\frac{3}{4\pi}z(x, y)\, dx\, dy$, where the factor 2 takes into account the mirror symmetry of the vesicle with respect to the $z = 0$ plane.
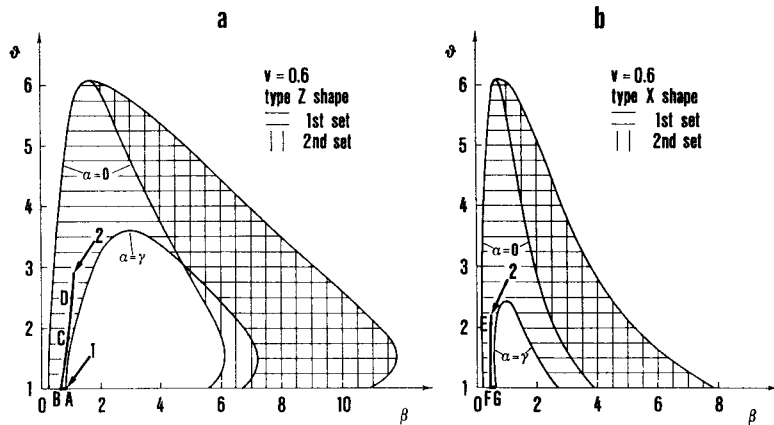
The type Z shapes have an elliptical top view in the xy plane, so the points having the same value of z lie on the ellipse with the semiaxis ratio ϑ (Fig. 1a). The vesicle surface is then expressed by the vector

$$R^Z = (x, y, f(\sqrt{x^2 + y^2/\vartheta^2})), \tag{8}$$

where $\vartheta \geq 1$ includes all shapes which can be generated. For the sake of convenience new coordinates ξ and t are introduced such that

$$x = \xi \cos t, \tag{9}$$

$$y = \xi\, \vartheta \sin t, \tag{10}$$

$$z = f(\xi). \tag{11}$$

It follows from (9)–(11) and (A1)–(A7) that

$$EG - F^2 = 1 + f_\xi^2 (\cos^2 t + \sin^2 t/\vartheta^2), \tag{12}$$

where f_ξ denotes the derivative of f with respect to ξ. The sum of the principal curvatures is

$$c_1 + c_2 \tag{13}$$
$$= \frac{(\cos^2 t + \vartheta^2 \sin^2 t + f_\xi^2)\,\vartheta f_\xi/\xi + (\sin^2 t + \vartheta^2 \cos^2 t)\,\vartheta f_{\xi\xi}}{[\vartheta^2 + f_\xi^2(\sin^2 t + \vartheta^2 \cos^2 t)]^{3/2}},$$

where $f_{\xi\xi}$ denotes the second derivative of f with respect to ξ. The element $dx\, dy$ is

$$dx\, dy = \vartheta \xi\, d\xi\, dt. \tag{14}$$

The type X shapes have an elliptical top view in the yz plane so that the points having the same value of x lie on the ellipse with the semiaxis ratio ϑ (Fig. 1b). The vesicle surface is then expressed by the vector

$$R^X = (x, y, \sqrt{f^2(x) - y^2/\vartheta^2}), \tag{15}$$

where $\vartheta \geq 1$ includes all shapes which can be generated. After introducing new coordinates such that

$$x = x, \tag{16}$$

$$y = \vartheta f(x) \cos t, \tag{17}$$

$$z = f(x) \sin t, \tag{18}$$

the expressions corresponding to (12)–(14) are

$$EG - F^2 = (f_x^2 + \sin^2 t + \cos^2 t/\vartheta^2)/\sin^2 t, \tag{19}$$

$$c_1 + c_2 = \frac{-1/(\vartheta^2 f) - (\cos^2 t + \sin^2 t/\vartheta^2)f_x^2/f + (\sin^2 t + \cos^2 t/\vartheta^2)f_{xx}}{(f_x^2 + \sin^2 t + \cos^2 t/\vartheta^2)^{3/2}} \tag{20}$$

and

$$dx\, dy = \vartheta f(x) \sin t\, dx\, dt, \tag{21}$$

where f_x denotes the derivative of f with respect to x and f_{xx} denotes the second derivative of f with respect to x.

The vesicle shape is characterized by its type (Z or X) and by four parameters α, β, γ and ϑ which are determined using three constraints for the membrane area, the enclosed volume, and the area difference of the two membrane leaflets (conditions (3)–(5)) and the equilibrium condition that the membrane bending energy is at its minimum. All the integrations are performed numerically within the intervals $t \in [0, 2\pi]$ and $\xi, x \in [0, \sqrt{\alpha^2 + \gamma^2}]$ using the Simpson method.

a

v = 0.6
type Z shape
— 1st set
| | 2nd set

b

v = 0.6
type X shape
— 1st set
| | 2nd set

Fig. 2 a, b. The region of possible values of parameter β and ϑ for the relative volume $v = 0.6$. **a** type Z shape, **b** type X shape. Different shadings represent different sets of shapes which are described in the text. The location of some characteristic equilibrium shapes depicted in Figs. 4 and 5 is marked with arrows and capital letters, respectively. The heavy lines represent β and ϑ values of the equilibrium shapes marked in Fig. 4
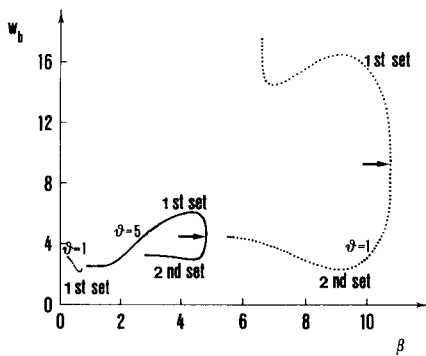

Fig. 3. Bending energy w_b as a function of the parameter β for two values of the parameter ϑ: $\vartheta = 1$ (*dotted lines*) and $\vartheta = 5$ (*full line*) for the type Z shapes. The arrows mark the points where the shapes of the first and the second set become identical

Results and discussion

The Cassini parameters α and γ are eliminated by satisfying conditions (3) and (4), which leaves the parameters β and ϑ undetermined at this point. All vesicle shapes having a simple closed surface which can be obtained by our procedure for a given membrane area and relative volume v, have values of β and ϑ within a bounded region in the (β, ϑ) plane. If $v = 1$, there is only one shape consistent with (3) and (4) for which $\beta = \vartheta = 1$ (sphere). By decreasing v, the size of the bounded region is increased. The bounded region of shapes for $v = 0.6$ is shown in Fig. 2 (marked by shading). The behavior of the system is also similar for other values of $v \in [0.6, 1]$. Both cases pertaining to the shape types Z and X, respectively, are considered (shown in Fig. 2a and b, respectively). Two sets of shapes can be obtained for each type; they are marked in Fig. 2 as the first and the second set of shapes, respectively. The left boundaries of both sets are determined by the condition $\alpha = 0$, i.e. when the shapes are ellipsoids. The two sets partially overlap, which means that some of the points in the bounded region correspond to one shape and some correspond to two shapes. For the points which correspond to two shapes (pertaining to the first and second set of shapes, respectively), the values of β and ϑ are identical, while the values of α and γ, the values of area difference of the two membrane leaflets and also the val-

ues of the membrane bending energies are different. At a given ϑ, the maximal possible value of β determines the right hand side of the bounded region where the shapes of the first and the second set become identical. This means that for the points on the right hand side boundary the values of all four parameters α, β, γ and ϑ, as well as the area difference of the two membrane leaflets and the membrane bending energy, are identical for the shapes of the first and the second set. At this value of the relative volume $v = 0.6$, a boundary exists for the shapes of the first set characterized by $\alpha = \gamma$, where the side view contour of these shapes is a lemniscate.

The dependence of the bending energy w_b on the parameter β for two values of parameter ϑ, i.e. for the axisymmetric shapes ($\vartheta = 1$; dotted lines) and for the non-axisymmetric shapes ($\vartheta = 5$; full line) for the type Z is shown in Fig. 3. It can be seen in Fig. 3 (and also in Fig. 2) that for $\vartheta = 1$ there is one shape for $\beta \in [0.33, 0.75]$ and for $\beta \in [5.5, 6.7]$. There are two shapes for $\beta \in [6.7, 10.75]$ while no shape exists for $\beta \in [0.75, 5.5]$. For $\vartheta = 5$ there is one shape for $\beta \in [0.68, 2.82]$ and two shapes for $\beta \in [2.82, 4.85]$. It can be seen in Fig. 3 how the shape of the first set is continuously connected to the shape of the second set at the maximal value of β for a given ϑ (marked with the arrow). Comparing our results with the results of the triparametric model used by Canham (1970) it should be noted that the shapes considered by Canham (1970) correspond to the first set of the type Z shapes for $\vartheta = 1$ and $\beta \in [0.33, 0.75]$.

By taking into account a constant value of the area difference of the two membrane leaflets (condition (5)), $\beta_{\Delta a}(\vartheta)$ lines can be defined in all sets of shapes in the bounded (β, ϑ) regions. An equilibrium shape for a given Δa is obtained by finding the values of parameters β and ϑ on such iso-Δa lines for which the value of the bending energy is minimal (denoted by $w_{b,equ}$). In some cases the value of ϑ is found to be $\vartheta = 1$, meaning that the equilibrium shape is axisymmetric.

Figure 4 shows the dependence of equilibrium shape energy $w_{b,equ}$ on Δa. We are considering ΔA values in the range where non-axisymmetric shapes could be expected, corresponding to the nearly spherical case (Heinrich et al. 1992) i.e. the range of ΔA values between the oblate and the prolate axisymmetric shapes with minimal energies. Elliptical shapes are marked with the full line while

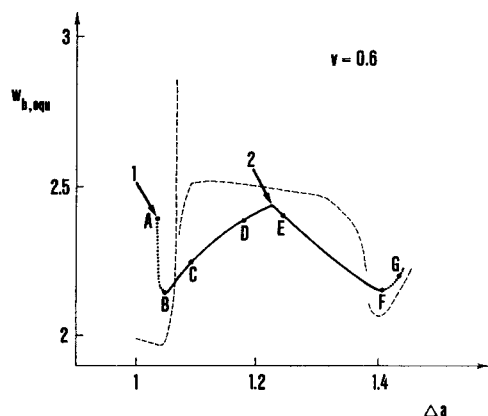Fig. 4. Bending energy of the equilibrium shapes $w_{b,\,equ}$ as a function of the area difference Δa for $v = 0.6$ calculated with the use of the four parametric model, and bending energy of the equilibrium shapes as a function of Δa, obtained by solving the general variational problem (*broken line*). The axisymmetric shapes obtained by the parametric model are represented by the *dotted line*, the elliptical shapes are represented by the *full line*. Bending energies of some characteristic equilibrium shapes depicted in Fig. 5 are marked with capital letters
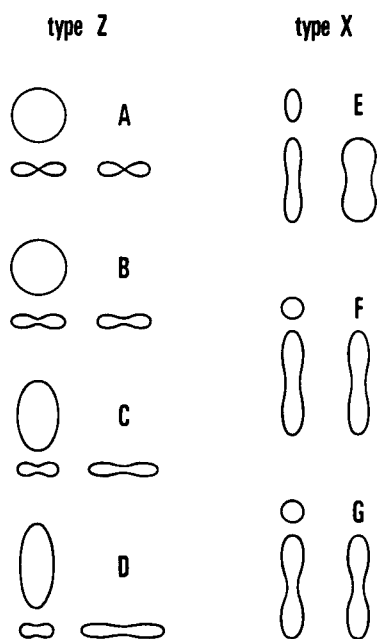

Fig. 5. Cross sections of some calculated shapes in all three perpendicular planes. The shapes are marked with capital letters corresponding to the ones used in Figs. 2 and 4. The orientations of the coordinate system for both types of shapes are as shown in Fig. 1

axisymmetric shapes are marked with the dotted line. Two intervals of Δa values can be seen, corresponding to two different types of equilibrium shapes. The interval within the bounds marked with arrows 1 and 2 involves the first set of shapes of type Z, while the interval extending beyond the bound marked with the arrow 2 involves the first set of shapes of type X. The values of the parameters β and ϑ of the shapes marked with the arrows in Fig. 4 are also depicted in the bounded (β, ϑ) region (Fig. 2) and marked with the corresponding arrows, re-

spectively. Some characteristic shapes are marked with capital letters to illustrate the change of shape as Δa changes; cross sections in all three perpendicular planes of the shapes marked in Fig. 4 are depicted in Fig. 5. As the curve in Fig. 4 is followed in the direction of increasing Δa, initially axisymmetric discoid shapes of the type Z (shapes marked with A and B) become elliptical, while the parameters β and ϑ increase as seen in Fig. 2 (shapes marked with C and D). If Δa is further increased, at the discontinuity of the derivative of the curve (point marked with the arrow 2) the shape changes abruptly into an elliptically symmetric dumbbell of the type X. If the curve is followed further on, the parameter ϑ of elliptically symmetric dumbbells (as the shape marked with E) decreases and reaches the value 1 (see Fig. 2) so that the shape becomes axisymmetric again. On a further increase of Δa, the axially symmetric dumbbells exhibit narrowing of the neck (shapes marked with F and G). The values of the parameters β and ϑ of the shapes marked in Fig. 4 are depicted in the (β, ϑ) plane (Fig. 2) and marked with the corresponding letters. In this analysis only shapes within a limited range of Δa values are considered. Outside this Δa range some rather peculiar equilibrium shapes, having very high membrane bending energies, are obtained. This results from the limitations of the parametric model and the evaluated shapes do not correspond to any of the observed shapes.

In Fig. 4 two local minima of the curve can be noted. The minimum at the lower Δa value gives an oblate discoid shape of the type Z, while the minimum at the higher Δa value gives a prolate dumbbell shape of the type X. It can also be shown that both local minima of the curve correspond to axisymmetric shapes. There is, however, a region of elliptical equilibrium shapes between the minima.

The results of our calculations are compared to the results obtained for axisymmetric shapes by solving the general variational problem i.e. the Euler differential equations for the principal curvatures, constrained by the conditions that the membrane area, the vesicle volume and the difference between the two membrane leaflet areas are fixed (Svetina and Žekš 1989). The membrane bending energy of the equilibrium shapes $w_{b,\,equ}$ as a function of Δa, calculated by solving the Euler equations, is also shown in Fig. 4 (broken line). Different segments of the dependence represent different classes of the shapes. Two local minima of the $w_{b,\,equ}$ (Δa) dependence can be noted. It was found (Svetina and Žekš 1989), that for the values of the relative volume v higher than about 0.65 the minimum pertaining to the higher value of Δa and corresponding to the prolate shape is energetically more favorable, while for lower values of v the minimum pertaining to the lower value of Δa and corresponding to oblate shapes is energetically more favorable. We found (not shown here) that the corresponding results of the parametric model agree with the results of the solution of the general variational problem. As expected, if only the axisymmetric shapes are considered, the energy calculated using the parametric model is higher than the corresponding value calculated with the use of the Euler equations for any Δa, owing to the lack of flexibility of the

parametric model compared to the exactness of the solution of the Euler equations. However, as can be seen in Fig. 4, if the elliptical shapes obtained by the parametric model are compared to axisymmetric solutions of the Euler equations, for some values of Δa between the two minima the elliptical shapes exhibit considerably lower energy. In this region of Δa the exact solution of the general variational problem for non-axisymmetric shapes must give even lower energy values than the ones we have obtained using the parametric model.

Comparing our results with the results of Sekimura and Hotani (1991), which indicate the existence of non-axisymmetric vesicle shapes for low values of the relative volume, our analysis differs from theirs as it takes into account elliptical shapes only while theirs takes into account various polygonal shapes. Sekimura and Hotani (1991), however, did not consider the prolate shapes (corresponding to the second set of the type Z shapes and also both sets of the type X shapes). Our analysis also includes the bilayer couple model which imposes on the system an additional constraint for the area difference of the two membrane leaflet areas Δa. It should be pointed out that, according to our results, non-axisymmetric shapes were obtained only for certain choices of Δa, while the absolute energy minimum was obtained for the axisymmetric shapes for all values of the relative volume between 0.6 and 1. Sekimura and Hotani (1991) obtained non-axisymmetric equilibrium shapes for low enough values of the relative volume as their function describing the top view contour yields different shapes than our strictly elliptical one. However, their equilibrium shape has, for a given v, higher energy than the corresponding equilibrium shape obtained by the exact solution of the general variational problem. In order to determine whether the absolute energy minimum is non-axisymmetric, an exact solution of the general variational problem for the non-axisymmetric shapes should be found.

The results of Heinrich et al. (1992) also indicate the existence of non-axisymmetric equilibrium shapes between the oblate and prolate axisymmetric shapes with an absolute minimum for axisymmetric shapes. The energy of the equilibrium non-axisymmetric shapes as a function of Δa does not exhibit any discontinuous derivatives such as seen in Fig. 4. We believe that the discontinuity in our $w_{b,\,\mathrm{equ}}(\Delta a)$ curve (point 2, Fig. 4) is a consequence of the limitations of the parametric model. It should be pointed out that the shapes obtained by Heinrich et al. (1992) are restricted to nearly spherical vesicles having the values of the relative volume v close to 1. Our results show that the non-axisymmetric equilibrium shapes can be continuously extended to considerably lower values of the relative volume, thereby proving the existence of a class of non-axisymmetric equilibrium shapes in the $v/\Delta a$ diagram. Our results indicate that the non-axisymmetric shapes appear in the $v/\Delta a$ diagram between the oblate and prolate axisymmetric shapes of minimal energy values. Starting in the region of oblate axisymmetric shapes at fixed relative volume v, the equilibrium shape energy decreases with increasing Δa and reaches its minimum within the class of oblate axisymmetric shapes. At this point, with a further increase of Δa, the equilibrium shape transforms continuously into a non-axisymmetric shape. After passing the interval of Δa of non-axisymmetric shapes, the shape again transforms continuously into a prolate axisymmetric shape in the point of minimum of bending energy within the class of prolate axisymmetric shapes. If Δa is increased still further in the region of prolate axisymmetric shapes, the energy of the equilibrium shapes increases.

It can be concluded that within the bilayer couple model for some values of Δa, non-axisymmetric shapes have lower energy values than any axisymmetric shape obtained at the same Δa values, which thereby proves the existence of stable non-axisymmetric shapes at these Δa values.

Appendix

The cell surface is represented by the vector $R = (x,\ y,\ z\,(x,\ y))$. It follows from the equations of differential geometry that the sum of the two principal curvatures c_1 and c_2 is expressed by

$$c_1 + c_2 = \frac{EN + GL - 2FM}{EG - F^2}, \tag{A1}$$

where

$$E = 1 + z_x^2, \tag{A2}$$

$$F = z_x z_y, \tag{A3}$$

$$G = 1 + z_y^2, \tag{A4}$$

$$L = \frac{z_{xx}}{(1 + z_x^2 + z_y^2)^{1/2}}, \tag{A5}$$

$$M = \frac{z_{xy}}{(1 + z_x^2 + z_y^2)^{1/2}}, \tag{A6}$$

$$N = \frac{z_{yy}}{(1 + z_x^2 + z_y^2)^{1/2}}, \tag{A7}$$

where the quantity Φ_α denotes the partial derivative of Φ with respect to α and the quantity $\Phi_{\alpha\beta}$ denotes the partial derivative of Φ with respect to α and β.

References

Canham PB (1970) The minimum energy of bending as a possible explanation of the biconcave shape of the human red blood cell. J Theor Biol 26:61–81

Deuling HL, Helfrich W (1976) The curvature elasticity of fluid membranes: A catalogue of vesicle shapes. J Phys (Paris) 37:1335–1345

Evans E (1974) Bending resistance and chemically induced moments in membrane bilayers. Biophys J 14:923–931

Heinrich V, Brumen M, Heinrich R, Svetina S, Žekš B (1992) Nearly spherical vesicle shapes calculated by use of spherical harmonics: axisymmetric and non-axisymmetric shapes and their stability. J Phys II France 2:1081–1108

Hotani H (1984) Transformation pathways of liposomes. J Mol Biol 178:113–120

Khodadad JK, Weinstein RS (1983) The band 3 – rich membrane of llama erythrocytes – studies on cell shape and the organization of membrane proteins. J Membr Biol 72:161–171

Lipowsky R (1991) The conformation of biomembranes. Nature 349: 475–481

Palek J (1987) Hereditary elliptocytosis, spherocytosis and related disorders: consequences of a deficiency or a mutation of membrane skeletal proteins. Blood Rev 1:147–168

Peterson MA (1985) An instability of the red blood cell shape. J Appl Phys 57:1739–1742

Peterson MA (1989) Deformation energy of vesicles at fixed volume and surface area in the spherical limit. Phys Rev A 39:2643–2645

Seifert U, Berndl K, Lipowsky R (1991) Shape transformations of vesicles: phase diagram for spontaneous – curvature and bilayer-coupling models. Phys Rev 44:1182–1202

Sekimura T, Hotani H (1991) The morphogenesis of liposomes viewed from the aspect of bending energy. J Theor Biol 149: 325–337

Sheetz MP, Singer SJ (1974) Biological membranes as bilayer couples. A mechanism of drug-erythrocyte interactions. Proc Natl Acad Sci, USA 71:4457–4461

Svetina S, Žekš B (1989) Membrane bending energy and shape determination of phospholipid vesicles and red blood cells. Eur Biophys J 17:101–111

Svetina S, Ottova-Leitmannova A, Glaser R (1982) Membrane bending energy in relation to bilayer couples concept of red blood cell shape transformations. J Theor Biol 94:13–23